VB studies on bonding features of HNC↔HCN

LIAO Xinli (　　　), WU Wei (　　　), MO Yirong (　　　)
& ZHANG Qianer (　　　)

Department of Chemistry, State Key Laboratory for Physical Chemistry of Solid Surfaces, Center for Theoretical Chemistry, Xiamen University, Xiamen 361005, China
Correspondence should be addressed to Wu Wei (email: weiwu@xmu.edu.cn)

Abstract   Within the bonded tableau unitary group approach (BTUGA), a scheme, combined with Pauling's resonance theory to select the predominant valence bond structures for VB calculations, is proposed. This scheme ensures a reliable and illustrative bonding picture in the description of chemical reactions, as exemplified by the isomerization reaction HNC↔HCN. The computation results account for important bonding features about this isomerization at the *ab initio* level and explore the mechanism of phenomena such as (i) HCN is more stable than HNC; (ii) the C-N bond first lengthens and then shortens in the vicinity of the transition state; (iii) only H-atom migration is observed in the isomerization process, without the breaking of the CN bond. Our results demonstrate that only a few bonded tableau functions are sufficient enough to provide a visual and reliable bonding picture.

The investigation on chemical reaction mechanism is one of the major activities and goals of the theoretical and computational chemistry. There have been considerable advances in recent years in developing high level methods to obtain accurate potential energy surface of small systems, which provides not only detailed information on the reaction path (energetic, geometric, and electronic properties) but also good starting points for the prediction of thermodynamic as well as kinetic properties. Nevertheless, molecular orbital (MO) theory has no insightful relations to valence-bond structures with which chemists have been familiar, and the compactness of wave functions is lost when a large scale configuration interaction (CI) is carried out in order to get an accurate energy profile. By contraries, the modern valence bond (VB) theory can provide a very physical and highly intuitive picture of bond breaking and bond making that occur in chemical reactions.

The co-existence of the two isomers has made HNC↔HCN a paradigm of H-atom migration, which is ubiquitous in chemical and biological processes. Moreover, this isomerization is the simplest case of the unimolecular reactions RNC↔RCN. Therefore, ever since the discovery of the stable, high energy isomer HNC in 1963, the isomerization HNC↔HCN has received extensive attention theoretically and experimentally[1—6]. However, it must be pointed out that the theo-

retical studies on this isomerization so far are restricted in the exploration of potential energy surfaces and minimum energy reaction paths, the automatic search of the transition structure, the evaluation of vibration energies, tunnel effect and correlation effect etc. Little attention is paid to a simple yet quantitative bonding picture for this isomerization. In this paper, therefore, based on the bonded tableau unitary group approach (BTUGA)[7−11] and Pauling's resonance theory[12], we offer a proposal for the classification of VB structures, and apply it to the study of the bonding features of the isomerization HNC ↔ HCN .

1   Methodology

1.1   Bonded tableau unitary group approach (BTUGA)[6,7]

As a simple spin-free VB method, BTUGA involves adopting bonded tableaus (BTs) as state functions of a system, where these state functions can describe resonance structures correspondingly. Thus, BTUGA is much closer to classical concepts and ideas than other many-body theories based on the molecular orbital theory. For an N-electron system, a BT is defined as

$$\boldsymbol{F}^{[I]}(k) = A_k e_{11}^{[I]} \boldsymbol{W}(k) = A_k e_{11}^{[I]}[u_1(1)u_2(2)\cdots u_n(n)], \tag{1}$$

where A_k is a normalization constant, $e_{11}^{[I]}$ is a standard projection operator for the irreducible representation $[I] = [2^{N/2-S}, 1^{2S}]$ of permutation group corresponding to the desired spin multiplicity $2S + 1$ and u_i is a one-electron basis function. Eq. (1) describes a VB structure where two one-electron basis u_{2i-1} and u_{2i} overlap to form a bond (i $N/2-S$ and the "bond" is a lone electron pair if $u_{2i-1} = u_{2i}$) and the last $2S$ one-electron functions are unpaired. Thus the wave function of the system can be expressed as a superimposition of all possible BTs, namely

$$\boldsymbol{Y}_i = \sum_{k=1}^{M} C_{ki} \boldsymbol{F}_i(k). \tag{2}$$

The structural weight of a BT $\boldsymbol{F}_i(k)$ in the $\boldsymbol{Y}_i$ can be defined as

$$T_i(k) = \sum_{l=1}^{M} C_{ik} C_{il} S_{kl}, \tag{3}$$

where S_{kl} is the overlap between the two BTs $\boldsymbol{F}_i(k)$ and $\boldsymbol{F}_i(l)$.

The condition of normalization requires

$$\sum_{i=1}^{M} T_i(k) = 1. \tag{4}$$

In the above equation, M is the number of linearly independent bonded tableaux,

$$M = \frac{(2S+1)[(m+1)!]^2}{(m+1)\left(\dfrac{N}{2}-S\right)!\left(m-\dfrac{N}{2}+S+1\right)!\left(m-\dfrac{N}{2}-S\right)!\left(\dfrac{N}{2}+S+1\right)!}, \tag{5}$$

where m is the number of one-electron orbitals.

The VB charge population $P(u_i)$ on the one-electron orbital u_i is defined as

$$P(u_i) = \sum_{k=1}^{M} T_i(k)m_i(k), \tag{6}$$

where $m_i(k) = 0$, 1, or 2, depending on whether the one-electron orbital u_i in the $\boldsymbol{F}(k)$ is filled with zero, one, or two electrons, respectively.

For the convenience of comparisons, we have defined a reduced potential energy function similar to that introduced by Bartlett et al.[13], namely

$$U(\boldsymbol{q}) = 1 + [E(\boldsymbol{q}) - E_{TS}] / D_0, \tag{7}$$

where $\boldsymbol{q}$ is the angle between R_{HC} and R_{CN}, defined as the reaction coordinate; $E(\boldsymbol{q})$ is the energy at $\boldsymbol{q}$ point of minimum energy path, E_{TS} is the energy of transition state, and $D_0 = E_{TS} - E_{HCN}$, i.e. the difference between the energy of transition state and the energy of HCN.

1.2   Computational details

Throughout this paper, Xiamen Package[14] was used for all VB calculations. 6-31G set was used, with the 1s orbitals of carbon and nitrogen being frozen to reduce the computational cost. Minimum energy path (MEP) was optimized at MP2/6-31G level and is listed in table 1, where R_{HC} and R_{NC} represent the H-C and C-N bond lengths, respectively. $\boldsymbol{q}$ is the angle between the two bonds H-C and C-N and defined as the reaction coordinate.

Table 1   Molecular geometries along the minimum energy path

Geometries	q / (°)	R_{HC}/nm	R_{CN}/nm	Geometries	q / (°)	R_{HC}/nm	R_{CN}/nm
A(HNC)	0 (HNC)	0.22059	0.12033	I	80	0.11683	0.12131
B	13	0.21481	0.12078	J	85	0.11502	0.12103
C	30	0.19194	0.12189	K	95	0.11229	0.12071
D	60	0.13050	0.12305	L	105	0.11050	0.12067
E	65	0.12559	0.12259	M	120	0.10884	0.12078
F(CHN)	67.929 (T.S.)	0.12335	0.12231	N	150	0.10733	0.12035
G	70	0.12195	0.12212	O	167	0.10707	0.11998
H	75	0.11913	0.12168	P (HCN)	180 (HCN)	0.10702	0.11984

1.3   Construction of valence bond wave functions

Consideration is restricted to the case of $S = 0$, and the numbers of one-electron function and valence electrons are nine and ten, respectively. Consequently, the total number of independent canonical VB structures is 5292 according to eq. (5). Atomic hybrid orbitals (AHOs) are taken as one-electron orbitals to ensure an unambiguous definition of a covalent or an ionic bond, and AHOs' expansion coefficients are simultaneously optimized with VB structural coefficients. In the following discussion, for simplicity, nine atomic hybrids are denoted with their dominant components as H(1s), C(s-p$_z$), C(p$_x$), C(p$_y$), C(s+p$_z$), N (s-p$_z$), N (p$_x$), N(p$_y$), N(s+p$_z$), and are denoted by Arabic numerals 1—9, respectively. The resultant zero spin means that singly occupied orbitals emerge in couples so that the electrons on these orbitals can couple with each other. At present,
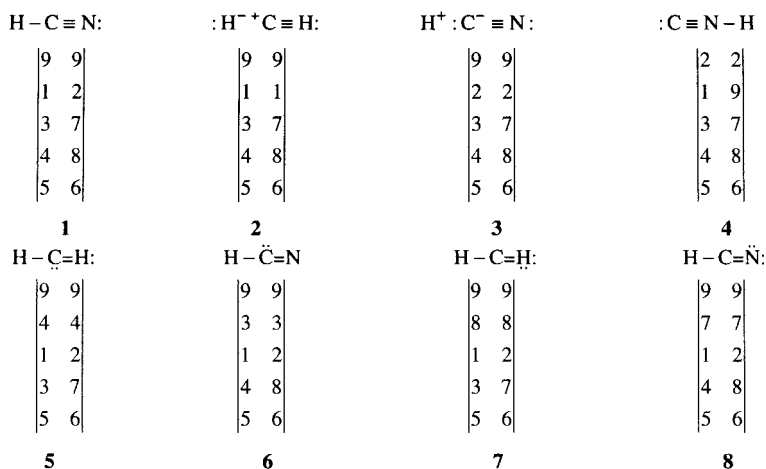
the possible numbers of singly occupied orbitals are 0, 2, 4, 6, and 8. For each of the cases, the numbers of independent VB structures are 126, 1260, 2520, 1260 and 126, respectively. As different VB structures make different contributions to various molecular states, it is valuable to find a minimum set of VB structures that can accurately describe a specific state. Subsequently, there are two questions. The first is that VB structures are necessary to be incorporated in the description of bonding behavior and the second question is how to choose them from thousands of resonance structures. Generally, the key to obtaining a clear and reliable bonding picture lies in selection of the predominant VB structures. To this end, we propose a scheme to make rational selection of VB-structures based on the Pauling's resonance theory [12]. The procedure is as follows:

(i) Excluding VB functions containing 0 or 2 singly occupied orbitals. Because the Pauling's electronegativities of H, C and N are 2.1, 2.5 and 3.0 respectively, it is more likely that there exist at least two covalent bonds in the HNC/HCN molecule. In other words, the resonance structures containing more than one covalent bond will make much more contribution to the real VB structure than those structures which contain no covalent bond or only one covalent bond.

(ii) Merely considering the VB functions that correspond to the classical covalent bonds. Those satisfying the above requirement are only five pairs whose singly occupied orbitals overlap to form bond. These five pairs include s bonds 1-2, 1-9, and 5-6, and π bonds 3-7 and 4-8.

(iii) According to other research work [15] and the contour lines of the 1BTSCF/OEOS calculation (that is, one BT function self-constituent field with overlap-enhanced orbitals as one-electron orbitals), there exists at least one π-bond between C and N atoms. Therefore, we conjecture that the predominant VB structures should be those containing at least one C-N π-bond. As a consequence, the favorable set of covalent bonds is obtained.

(iv) To ensure the accuracy, we repeat test calculations at three critical geometries (HNC, HCN, TS) and iteratively adjust the selection until three energy values are accurate enough. Eventually, we pick out 31 BT functions, as shown in fig. 1, to carry out VB calculations for the whole energy profile.
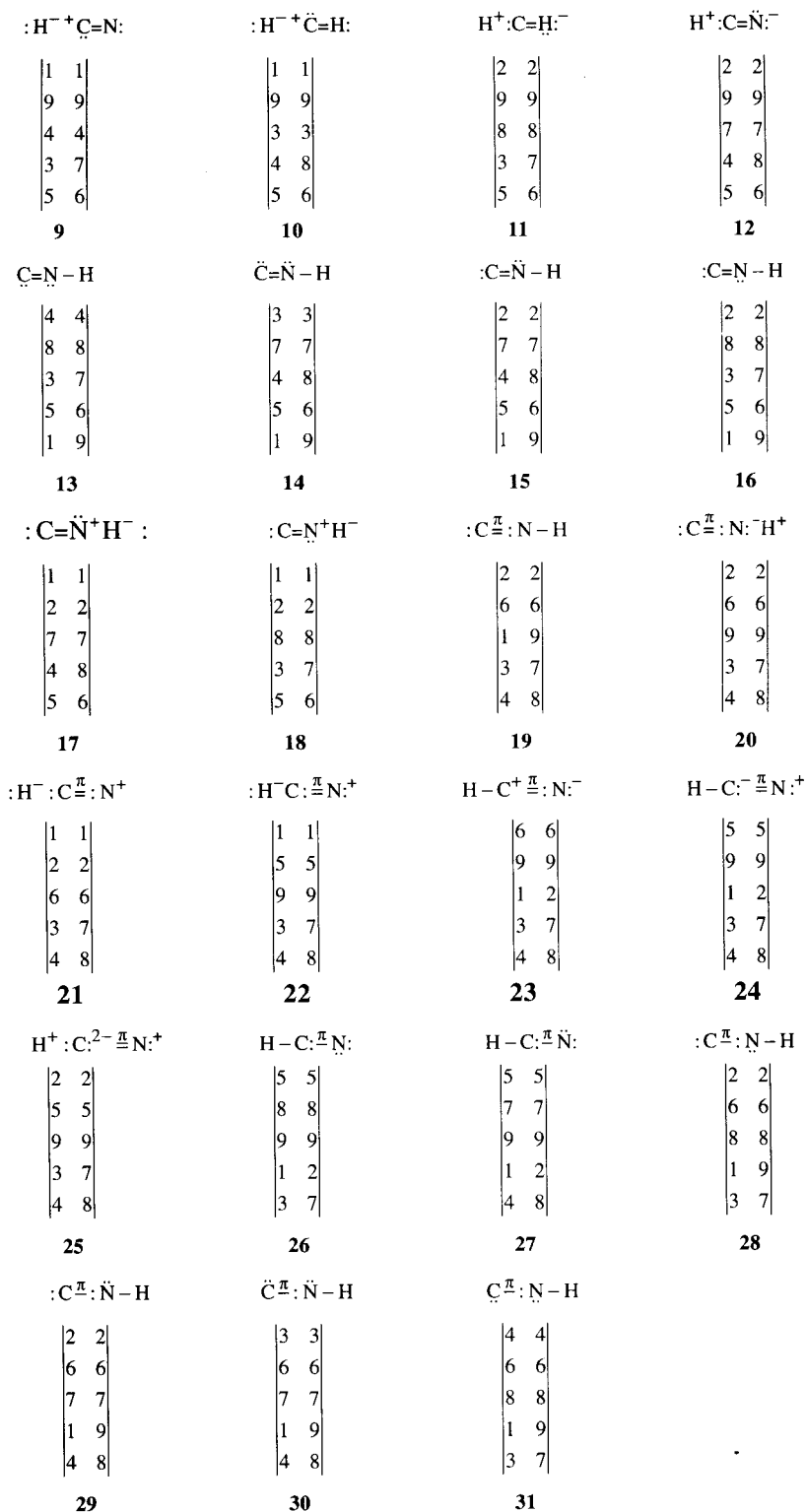
$:H^{-+}\overset{..}{C}=N:$

$$\begin{vmatrix} 1 & 1 \\ 9 & 9 \\ 4 & 4 \\ 3 & 7 \\ 5 & 6 \end{vmatrix}$$

9

$:H^{-+}\overset{..}{C}=H:$

$$\begin{vmatrix} 1 & 1 \\ 9 & 9 \\ 3 & 3 \\ 4 & 8 \\ 5 & 6 \end{vmatrix}$$

10

$H^{+}:C=H:^{-}$

$$\begin{vmatrix} 2 & 2 \\ 9 & 9 \\ 8 & 8 \\ 3 & 7 \\ 5 & 6 \end{vmatrix}$$

11

$H^{+}:C=\overset{..}{N}:^{-}$

$$\begin{vmatrix} 2 & 2 \\ 9 & 9 \\ 7 & 7 \\ 4 & 8 \\ 5 & 6 \end{vmatrix}$$

12

$\overset{.}{C}=\overset{.}{N}-H$

$$\begin{vmatrix} 4 & 4 \\ 8 & 8 \\ 3 & 7 \\ 5 & 6 \\ 1 & 9 \end{vmatrix}$$

13

$\overset{..}{C}=\overset{.}{N}-H$

$$\begin{vmatrix} 3 & 3 \\ 7 & 7 \\ 4 & 8 \\ 5 & 6 \\ 1 & 9 \end{vmatrix}$$

14

$:C=\overset{.}{N}-H$

$$\begin{vmatrix} 2 & 2 \\ 7 & 7 \\ 4 & 8 \\ 5 & 6 \\ 1 & 9 \end{vmatrix}$$

15

$:C=N-H$

$$\begin{vmatrix} 2 & 2 \\ 8 & 8 \\ 3 & 7 \\ 5 & 6 \\ 1 & 9 \end{vmatrix}$$

16

$:C=\overset{..}{N}^{+}H^{-}:$

$$\begin{vmatrix} 1 & 1 \\ 2 & 2 \\ 7 & 7 \\ 4 & 8 \\ 5 & 6 \end{vmatrix}$$

17

$:C=N^{+}H^{-}$

$$\begin{vmatrix} 1 & 1 \\ 2 & 2 \\ 8 & 8 \\ 3 & 7 \\ 5 & 6 \end{vmatrix}$$

18

$:C\overset{\pi}{\underset{=}{}}:N-H$

$$\begin{vmatrix} 2 & 2 \\ 6 & 6 \\ 1 & 9 \\ 3 & 7 \\ 4 & 8 \end{vmatrix}$$

19

$:C\overset{\pi}{\underset{=}{}}:N:^{-}H^{+}$

$$\begin{vmatrix} 2 & 2 \\ 6 & 6 \\ 9 & 9 \\ 3 & 7 \\ 4 & 8 \end{vmatrix}$$

20

$:H^{-}:C\overset{\pi}{\underset{=}{}}:N^{+}$

$$\begin{vmatrix} 1 & 1 \\ 2 & 2 \\ 6 & 6 \\ 3 & 7 \\ 4 & 8 \end{vmatrix}$$

21

$:H^{-}C\overset{\pi}{\underset{=}{}}:N:^{+}$

$$\begin{vmatrix} 1 & 1 \\ 5 & 5 \\ 9 & 9 \\ 3 & 7 \\ 4 & 8 \end{vmatrix}$$

22

$H-C^{+}\overset{\pi}{\underset{=}{}}:N:^{-}$

$$\begin{vmatrix} 6 & 6 \\ 9 & 9 \\ 1 & 2 \\ 3 & 7 \\ 4 & 8 \end{vmatrix}$$

23

$H-C:^{-}\overset{\pi}{\underset{=}{}}N:^{+}$

$$\begin{vmatrix} 5 & 5 \\ 9 & 9 \\ 1 & 2 \\ 3 & 7 \\ 4 & 8 \end{vmatrix}$$

24

$H^{+}:C:^{2-}\overset{\pi}{\underset{=}{}}N:^{+}$

$$\begin{vmatrix} 2 & 2 \\ 5 & 5 \\ 9 & 9 \\ 3 & 7 \\ 4 & 8 \end{vmatrix}$$

25

$H-C:\overset{\pi}{\underset{=}{}}\overset{.}{N}:$

$$\begin{vmatrix} 5 & 5 \\ 8 & 8 \\ 9 & 9 \\ 1 & 2 \\ 3 & 7 \end{vmatrix}$$

26

$H-C:\overset{\pi}{\underset{=}{}}\overset{..}{N}:$

$$\begin{vmatrix} 5 & 5 \\ 7 & 7 \\ 9 & 9 \\ 1 & 2 \\ 4 & 8 \end{vmatrix}$$

27

$:C\overset{\pi}{\underset{=}{}}:N-H$

$$\begin{vmatrix} 2 & 2 \\ 6 & 6 \\ 8 & 8 \\ 1 & 9 \\ 3 & 7 \end{vmatrix}$$

28

$:C\overset{\pi}{\underset{=}{}}:\overset{.}{N}-H$

$$\begin{vmatrix} 2 & 2 \\ 6 & 6 \\ 7 & 7 \\ 1 & 9 \\ 4 & 8 \end{vmatrix}$$

29

$\overset{..}{C}\overset{\pi}{\underset{=}{}}:\overset{.}{N}-H$

$$\begin{vmatrix} 3 & 3 \\ 6 & 6 \\ 7 & 7 \\ 1 & 9 \\ 4 & 8 \end{vmatrix}$$

30

$\overset{.}{C}\overset{\pi}{\underset{=}{}}:\overset{.}{N}-H$

$$\begin{vmatrix} 4 & 4 \\ 6 & 6 \\ 8 & 8 \\ 1 & 9 \\ 3 & 7 \end{vmatrix}$$

31

Fig. 1.   Selected VB structures and their corresponding BT functions for VB calculations.

2   Results and discussion

2.1   Energies

At the level of 31BTSCF/AHOs, the energies of HNC and HCN are −92.884724 and −92.918340 a.u., respectively, which are significantly lower than that at the HF level (−92.811472 and −92.821110 a.u.), indicating that the selected 31BTs can recover considerable amount of electron correlation and provide a proper description of the isomerization of HNC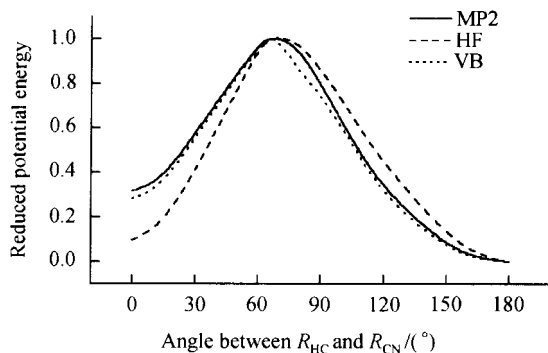/HCN. Our isomerization energy is 88.1562 kJ/mol, comparable with the value 95.8474 kJ/mol at the MP2 level but higher than the experimental data of (61.864 ± 0.836) kJ/mol[16]. Fig. 2 shows the reduced energy curves computed at 31BTSCF, MP2 and HF levels. The reduced energy curve of 31BTSCF almost coincides with that of MP2 except for the bending configurations where $q = 60°—100°$, while there is an obvious discrepancy between the curves at the MP2 and HF levels in the entire

Fig. 2.   Reduced potential energies versus the reaction coordinate θ, from the 31BTSCF, MP2 and HF calculations.

reaction process. Thus, although potentially larger basis sets and more VB structures can further improve computational results, we believe that the selected 31BTs can provide a satisfactory VB description as our focus is on the bonding picture instead of on the accuracy of energy.

2.2   VB structural weights

The weights of various VB structures for different nuclear configurations are calculated. At the equilibrium geometry of HNC, it is found that only five structures (i.e. **11**, **12**, **15**, **16**, and **19**) have the weights larger than 0.1, while the weights of structures **3** and **4** are about 0.03—0.04. This indicates that the nature of the C-N bond is more likely to be double instead of being triple as suggested traditionally. As the reaction proceeds forward, the contributions from structures **11**, **12** and **19** reduce gradually, whereas structures **18** and **28** get more and more important. For the D nuclear configuration, the weights of structures **15** and **16** become zero abruptly, while the contribution from structure **1** obviously increases. After the D configuration, the structures **1—3**, **5—10**, **21**, **26** and **27** start to dominate the description of the isomerization gradually. At the equilibrium geometry of HCN, structure **1**   H − C ≡ N: plays the most important role with a weight of 0.19, larger than that of structure **4** in the nuclear configuration A, implying that σ-interaction between C and N atoms may be stronger in the HCN molecule than that in the HNC molecule. This observation explains the origin why HCN is more stable than HNC and why the C-N bond length in HCN is shorter than that in HNC.

2.3   Further VB analysis

2.3.1   H-C and H-N bonds.   According to the characteristic of the H-C and H-N bonds, the 31BTs are classified into six groups, denoted as H-C, H^-C^+, H^+C^-, H-N, H^-N^+, and H^+N^-. The calculations show that the contribution of H^+C^- to the ground state of the molecular system is always larger than that of H^-C^+, and that the weight of H^+N^- is also larger than that of H^-N^+ in the entire isomerization process. These results not only agree very well with Pauling's electronegativity rule, but also show that the selected 31BTs can provide an appropriate bonding picture. Furthermore, the structural weight of the H-N covalent bond is 0.638 for the HNC molecule, while the weight of H-C covalent bond is 0.705 for the HCN molecule. For further comparisons, we define the weight difference between H^+A^- and H^-A^+ (H^+A^- -H^-A^+) as the contribution of ionic bond. Hence, the ionic character of the H-C bond is 0.064, and that of the H-N bond is 0.290. By normalizing the structural weights, we have the covalent character of 0.917 for the H-C bond in HCN, and the corresponding value for the H-N bond in HNC is 0.688. This indicates that the H-C bond of the HCN molecule has much more covalent character than the H-N bond of the HNC molecule. In other words, the H-C bond of HCN will be more stable than the H-N bond of HNC. This provides another explanation for the fact that the HCN molecule is more stable than the HNC molecule.

Fig. 3 shows also the variation of the structural weights of the H-C and H-N bonds vs. the reaction coordinate q. It is seen that the weight of the H-C bond increases almost monotonically, showing that the H-C bond becomes strong as the reaction proceeds. On the contrary, the interaction between the H and N atoms tends to become weak in the $HNC \rightarrow HCN$ process. In addition, an abrupt variation occurs in the range from $q = 30°$ to $q = 75°$. This indicates that the H-C bond is formed while the H-N bond is broken in the vicinity of the transition state.

Fig. 3.   Variations of structure weights of H-C and H-N bonds versus the reaction coordinate θ, i.e. the angle between R_{HC} and R_{CN}.

2.3.2   C-N bond.   To investigate the behavior of the C-N bond, the selected 31VB structures are regrouped into six types according to the feature of the C-N bond, which are denoted as $C \equiv N, C^+ = {}^-N$ or $C^- = {}^+N$, H-C = N, C = N-H, $C \overset{\partial}{=} N$ and $C \overset{\partial}{-} N$. The weights of each type of VB structures along MEP are given in table 2. It is found that the structural weight of $C \equiv N$ increases almost monotonously in the process of the isomerization reaction $HNC \rightarrow HCN$. At the HNC equilibrium geometry, the weight of the VB structures containing $C \equiv N$ is only 0.07, while the corresponding value at HCN equilibrium geometry is 0.31, showing that the structure weigh of $C \equiv N$ in the molecule HCN is 0.22, larger
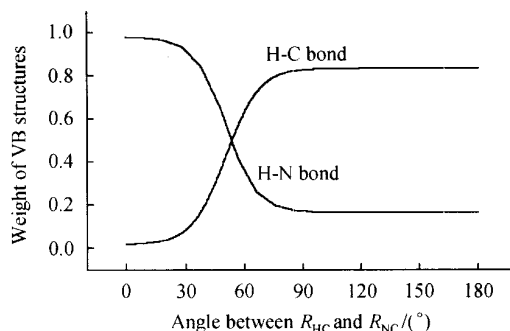
than that in HNC. Since the triplet bond consists of double π-bond and single σ-bond, the higher weight of $C \equiv N$ means a stronger σ-interaction. In other words, the σ-bonding between C and N in the HCN molecule is stronger than that in HNC. Furthermore, if the contribution of the ionic bond is taken into account, that is, the VB structural weight of the first type is combined with that of the second type, then the structural weight of the triplet C-N bond in HCN becomes 0.471, which is by 0.389 larger than that in HNC. Therefore, we can conclude that the larger structural weight of the triplet C-N bond and stronger σ-interac- tion of HCN account for the fact that the C-N bond length of HCN is shorter than that of HNC and that HCN is more stable than HNC.

    The results for the third, forth and fifth types of the C-N bond have further confirmed the above conclusions. In addition, the calculated results for the sixth type C-N bond provide new information about the behavior of the C-N bond. The results show that the weight of $C \overset{\pi}{-} N$ is 0.192 for HNC, and the corresponding value is 0.130 for HCN. In the isomerization process, the value of the structural weight first increases until the configuration G and then shows a tendency to reduce from configuration H to HCN configuration. This behavior is similar to that of the C-N bond length variation in the reaction, as the C-N bond-length first becomes long and then tends to become short in the vicinity of the transition state. This indicates that there is a correlation be- tween the interaction of the π-electrons and the C-N bond length. When the weight of the π-bond is large, the bond is weak, and subsequently the bond length is long. By contraries, when the interactions of the σ-electrons become important, the C-N bond gets strong and the C-N bond length shortens.

Table 2   Weights of various C-N bonds

Config./Struct.	$C \equiv N$	$C^{+}=\overset{-}{N}$ $C^{-}=\overset{+}{N}$	H-C = N	C = N-H	$C \overset{\pi}{=} N$	$C \overset{\pi}{-} N$
A(HNC)	0.070	0.012	−0.002	0.523	0.205	0.192
B	0.073	0.012	−0.002	0.523	0.199	0.194
C	0.080	0.011	0.000	0.524	0.190	0.194
D	0.251	0.014	0.262	0.127	0.120	0.226
E	0.257	0.027	0.266	0.129	0.097	0.224
F(CHN)	0.250	0.033	0.269	0.133	0.092	0.223
G	0.258	0.039	0.282	0.127	0.063	0.230
H	0.269	0.045	0.289	0.116	0.064	0.217
I	0.271	0.050	0.301	0.115	0.054	0.210
J	0.271	0.052	0.299	0.119	0.060	0.200
K	0.274	0.057	0.311	0.114	0.057	0.187
L	0.274	0.072	0.301	0.112	0.061	0.181
M	0.280	0.080	0.316	0.095	0.047	0.182
N	0.300	0.161	0.245	0.087	0.064	0.142
O	0.308	0.171	0.237	0.089	0.067	0.128
P(HCN)	0.305	0.166	0.246	0.086	0.067	0.130

2.3.3   Charge distribution.   To check the atomic population distribution in the reaction, the variation of population on H, C and N versus the reaction coordinate q is plotted in fig. 4. It is seen from fig. 4 that the electron population on hydrogen increases rapidly in the range of q =

0°—80° and afterwards increases slowly. For carbon, the variation of atomic population is divided into four periods: the population increases slowly during $q = 0°$—30°, and then raises rapidly in the range of $q = 30°$—67°. In the range of $q = 67°$—120°, the value oscillates at 4.00, indicating that carbon is neutral after adding the 2 core electrons up. After that, there is an obvious increase of the charges on carbon. In contrast with hydrogen and carbon, the value of nitrogen decreases monotonously in the entire process, showing that the electrons are transferred from N to H and from N to C. For nitrogen, the value reduces steeply when $q = 30°$—67°, but the variation is slow in the range of $q = 67°$—180°. This indicates that the charge transfer is fast before reaching at the transition state, and the charge transfer mainly occurs in the range of $q = 30°$—67°, i.e. the vicinity of the transition state. After reaching the transition state, the charge transfer becomes slow. At the equilibrium geometry of HCN, the charge distributions are H(+0.167e), C(−0.041e) and N(−0.126e) respectively, which is in agreement with Pauling's electronegativity rule.
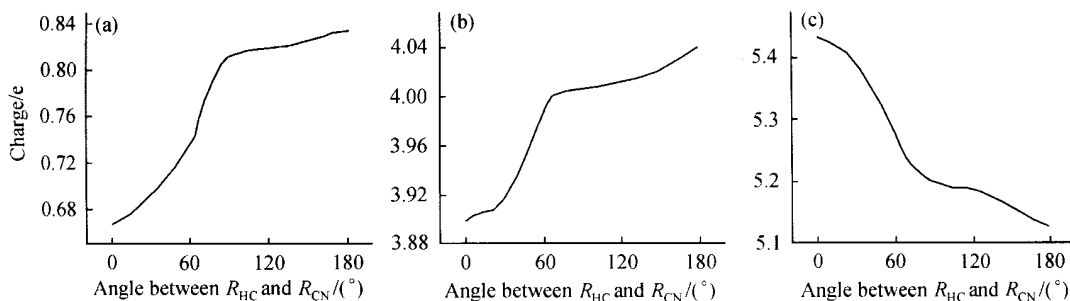

Fig. 4.　Variation of charges on (a) hydrogen, (b) carbon, and (c) nitrogen versus the reaction coordinate θ, i.e. the angle between R_{HC} and R_{CN}.

3　Conclusions

In this paper a simple scheme, combined with Pauling's resonance theory, to choose and construct the VB wave function has been proposed. By following the procedure to make a rational selection of predominant VB structures, only a few bonded tableau functions are capable of recovering considerable amount of correlation energy. The bonding features of the bonds H-C, H-N, and C-N along MEP are elaborately discussed. The calculation results can provide a plausible explanation for the facts that the HCN is more stable than the HNC and the C-N bond first lengthens and then shortens in the vicinity of the transition state.

References

1. Skurski, P., Gutowski, M., Simons, J., *Ab initio* electronic structure of HCN- and HNC-dipole-bound anions and a description of electron loss upon tautomerization, J. Chem. Phys., 2001, 114(17): 7443—7449.
2. Jursic, B. S., Complete basis set *ab initio* study of potential energy surfaces of the dissociation recombination reaction HCNH++e(-), J. Mol. Struct., 1999, 487(3): 211—220.
3. Abashkin, Y., Russo, N., Toscano, M., Transition states and energy barriers from density functional studies: representative

isomerization reactions, Int. J. Quantum Chem., 1994, 52: 695—704.

4. Bentley, J. A., Bowman, J. M., Gazdy, B. et al., A global *ab initio* potential for HCN/HNC exact vibrational energies and comparision to experiment, Chem. Phys. Lett., 1992, 198(6): 563—569.

5. Bentley, J. A., Huang, C. M., Wyatt, R. E., Highly vibrationally excited HCN/HNC: eigenvalues, wave functions, and stimulated emission pumping spectra, J. Chem. Phys., 1992, 98(7): 5207—5221.

6. Peric, M., Mladrenovic, M., Peyerimhoff, S. D. et al., *Ab initio* study of the isomerization HNC-HCN, 1. *Ab initio* calculation of the HNV reversible HCN potential surface and the corresponding energy-levels, Chem. Phys., 1983, 82: 317—336.

7. Zhang, Q. E., Li, X. Z., Bonded tableau method for many-electron systems, J. Mol. Struct. (Theochem.), 1989, 198: 413—425.

8. Li, X. Z., Zhang, Q. E., Bonded tableau unitary group approach to the many-electron correlation problem, Int. J. Quantum Chem., 1989, 36: 599–632.

9. Li, J. B., Wu, W., New algorithm for nonorthogonal *ab initio* valence-bond calculations, Theor. Chim. Acta, 1994, 89: 105—121.

10. Wu, W., Mo, Y. R., Zhang, Q. E., On the resonance theory, J. Mol. Struct., 1993, 283: 227—236.

11. Mo, Y. R., Wu, W., Zhang, Q. E., Valence bond description for the ground state and several low-lying excited states of LiH, J. Mol. Struct., 1993, 283: 237—249.

12. Pauling, L., The Nature of Chemical Bond, 3rd ed., Ithaca, New York: Cornell University Press, 1960, 64–107.

13. Sosa, C., Noga, J., Purvis, G. D. et al., An application of the full CCSDT coupled-cluster method to potential-energy curves—— the CH_4 CH_3+H dissociation, Chem. Phys. Lett., 1998, 153(2-3): 139—146.

14. Wu, W., Song, L. C., Mo, Y. R. et al., XIAMEN——An *ab initio* Spin-Free Valence Bond Program, Xiamen: Xiamen University, 1999.

15. Li, Q. M., Fu, X. Y., The topological characteristics of the structures in the vicinity of the transition state of HCN-HNC isomerization, Acta Phys. Chem. Sinica (in Chinese), 1992, 8(6): 724–727.

16. Pau, C. F., Hehre, W. J., Heat of formation of hydrogen isocyanide by ion-cyclotron double-resonance spectroscopy, J. Phys. Chem., 1982, 86(3): 321—322.